Conductive-AFM Patterning of Organic Semiconductors

Benjamin P. Brown, Loren Picco, Mervyn J. Miles, and Charl F. J. Faul**

The atomic force microscope (AFM) has developed into a mature and widespread topography characterisation tool since its inception in the 1980s. The high resolution and precision nature of this tool has also led to widespread use, under ambient conditions, for diverse applications. These applications include the direct observation of single-molecule events,[1,2] molecular force measurements,[3,4] the fabrication of nanostructures via a variety of nanoscale lithographies,[5,6] including electrochemical deprotection to yield responsive monolayers,[7,8] enzymatic oxidative polymerization to locally form conducting polymers,[9] formation of polymerized sulphur nanostructures,[10] and direct writing of metallic nanostructures.[11] These applications were recently classified into mechanical, thermal, diffusive, and electrical processes according to the dominant tip–surface interaction involved.[12] The last includes probe-based oxidation and reduction lithographies. Although oxidative processes are known, and have been exploited extensively,[13–15] reductive processes under ambient conditions are less common.

Here we show, in a facile single-step approach, reversible local reductive and oxidative patterning of thin films of an electroactive organic material performed with a commercial conductive AFM (c-AFM) under ambient conditions. This constructive nanolithography[16] approach locally modifies the top layer of the organic thin film without inducing any of the topographic or structural changes typical of "destructive" local-oxidation nanolithography techniques.[17,18] This constructive c-AFM redox-writing (cAROW) methodology shows potential for further exploration and development into a scalable, fast write-read technology.[19,20]

The organic semiconductor used in this investigation is based on phenyl/amine-capped tetra(aniline), **Ph/NH$_2$-TANI**, a short-chain, functional, and well-defined low molecular weight oligomeric analogue of the well-known conducting polymer, poly(aniline), PANI. **Ph/NH$_2$-TANI** retains the desirable optoelectronic properties of PANI while circumventing the issues of poor solubility, processability, and polydispersity that have previously limited the applications of the polymer.[21] It is possible to fine-tune the optoelectronic properties of tetra(aniline) derivatives, and higher oligomers, simply through modification of the central unit and variation of the end-group functionalization.[22] Similar to PANI, these oligomeric materials can be reversibly switched (doped) from their conductive emeraldine salt (ES) state to either the non-conductive fully reduced leucoemeraldine base (LEB) or emeraldine base (EB) states through redox, and acid–base chemistry, respectively.[23] An extensive range of possible inorganic and organic acid dopants exists, with the latter able to simultaneously act as dopants and plasticisers.

In this work, *N*-(4-(((1E,4E)-4-((4-(phenylamino)-phenyl)imino)-cyclohexa-2,5-dien-1-ylidene)amino)phenyl)octanamide (**TANI-C$_8$**) doped to the conductive ES state with the prototypical PANI dopant camphorsulfonic acid (**CSA**) was chosen, as this combination formed smooth, continuous thin films on highly oriented pyrolytic graphite (HOPG). Unlike EB-state **TANI**-based materials,[24] films prepared from ES-state **TANI-C$_8$** (see the Experimental Section for details)

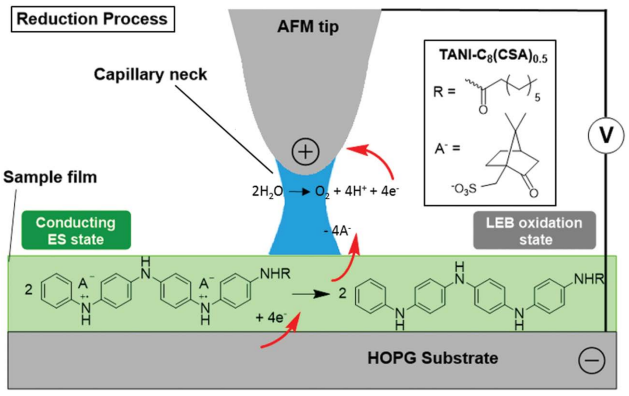

Scheme 1. cAROW reduction of TANI-C$_8$(CSA) from the ES state to the LEB state. Electroneutrality is maintained through ion exchange with water either adsorbed onto the film or within the meniscus between the AFM tip and sample. Red arrows show charge transfers.

Dr. B. P. Brown, Prof. C. F. J. Faul
School of Chemistry
University of Bristol
Bristol BS8 1TS, UK
E-mail: charl.faul@bristol.ac.uk
Dr. B. P. Brown
Bristol Centre for Functional Nanomaterials
Centre for Nanoscience and Quantum Information
University of Bristol
Tyndall Avenue, Bristol BS8 1FD, UK
Dr. L. Picco, Prof. M. J. Miles
School of Physics
University of Bristol
Bristol BS8 1TL, UK
E-mail: m.j.miles@bristol.ac.uk
Dr. L. Picco, Prof. M. J. Miles
Centre for Nanoscience and Quantum Information
University of Bristol
Bristol BS8 1FD, UK

DOI: 10.1002/smll.201501779

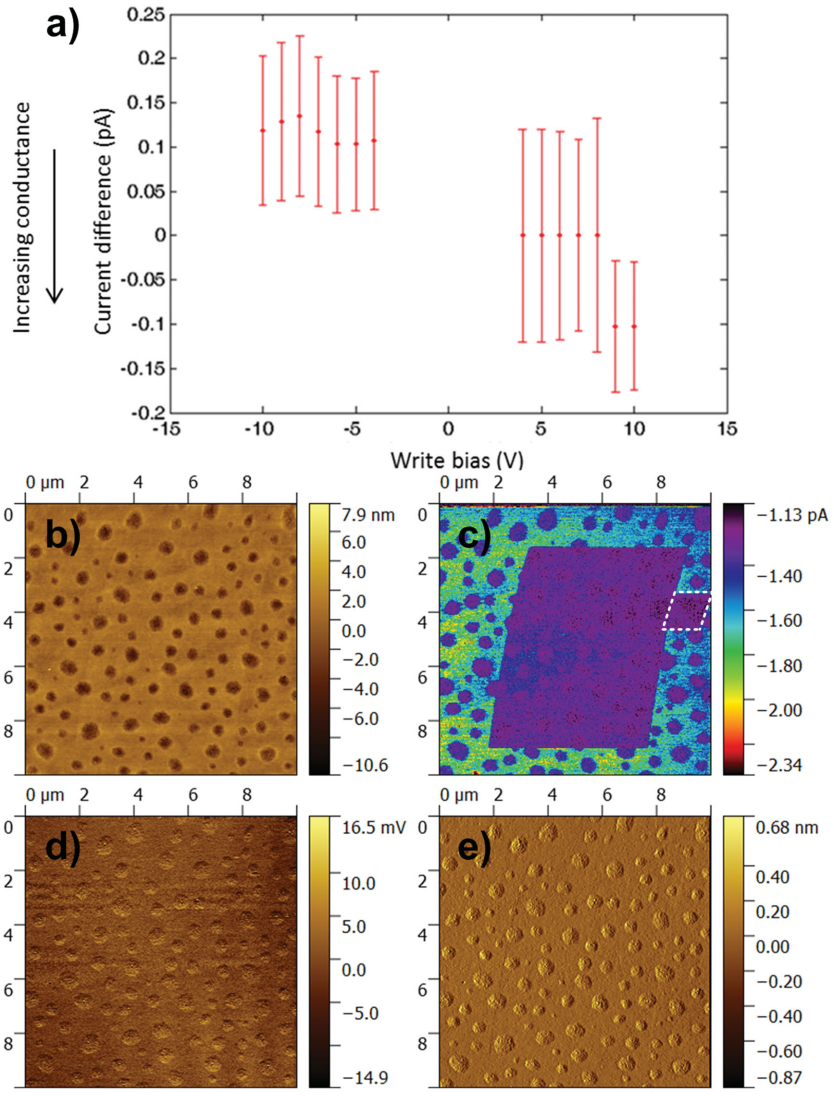

Figure 1. a) Plot of effect of different write biases. Area was scanned with a set write bias then reimaged with a bias of –6 V. Current difference is the difference in current through the written area before and after write scan, note a positive current difference implies the written feature is less conductive than the as-prepared film; b) AFM height c) current, d) friction, and e) deflection images of a written area. The area indicated with the white dashed box in (c) is from a previous smaller scan (–6 V bias); the height features that can be seen in the film were attributed to solvent evaporation during the film-forming process and are discussed in more detail in Section 2 of the Supporting Information.

were typically ≈20 nm thick, with continuous areas of greater than 100 × 100 μm^2 possessing a root mean square (RMS) roughness of 0.47 nm. **Scheme 1** gives an overview of the AFM redox-writing process developed in this work.

As proof-of-concept, we scanned these thin films using the c-AFM mode of the microscope with a range of bias voltages from –10 to +10 V (**Figure 1**a). Scanning areas of the conductive ES **TANI-C$_8$** film, while a tip–sample bias of –4 to –10 V was applied, led to a reduction in the current flow through the film during subsequent scans of the same area, indicating that the first scan had induced a change in the conductance of the film. This effect was not observed after scanning with positive biases (+4 to +10 V) and was only observed when reimaging the scanned area with a negative bias (–4 to –10 V). Biases greater than ±8 V were sometimes found to induce damage to the surface of the thin film, as evidenced by the increase in conductance for +9 and +10 V write biases in Figure 1a. As shown by the work of Hoeppener et al.[16,18] these topographic and structural alterations could be due to deterioration of the organic film when exposed to sufficiently high voltage bias or increased tip-sample interaction forces due to increased attractive electrostatic forces during writing. By keeping the bias within the range from –10 to +10 V and with careful refinement of the contact-mode AFM height feedback loop, it was found that the conductance of the films could be modified without any associated physical change in the film evident in the AFM height, deflection or friction data (Figure 1b–e, see the Supporting Information for further examples), suggesting that the modifications are electrochemical in nature and result in a change in the conductivity of the film. The observed change in conductivity of the film is consistent with the area of substrate underneath the tip being reduced to nonconductive LEB **TANI-C$_8$** when scanned with negative biases, and no reaction occurring with positive biases (as there is no direct oxidative route to a nonconductive state of **TANI-C$_8$**). The data in Figure 1 also provide evidence that any changes in conductivity are unlikely to be the result of a change in the physical structure of the film due to joule heating by the probe, as this effect would be unaffected by the polarity of the bias. During optimization of writing conditions, we found that a bias voltage of –6 V offered reliable writing within a single pass while minimizing any perturbation of the film surface (Figure 1).[25]

In solution, the chemical reduction of ES **TANI** to LEB **TANI** is highly reversible (and one of the attractive features of aniline-based materials). Such switchable behaviour thus presents a potential route toward multiple write/read/erase cycles in our cAROW approach. Encouragingly, initially scanning an area of written nonconductive LEB **TANI** with a positive bias of between +6 and +10 V oxidises the material back to the conductive ES state, thus erasing the written feature. The repeatable nature of this LEB to ES to LEB cycle is shown in **Scheme 2** where the surface is taken from LEB to ES and back to the LEB state twice. Initially, a 15 × 7.5 μm^2 area of ES-state **TANI-C$_8$** was written to the nonconducting LEB state with a reductive –6 V bias. A 6 × 3.75 μm area was then converted to the conducting ES state with a +6 V (oxidative) bias (Step 1). The original 15 × 7.5 μm area was read with a –6 V bias (Step 2).

www.MaterialsViews.com

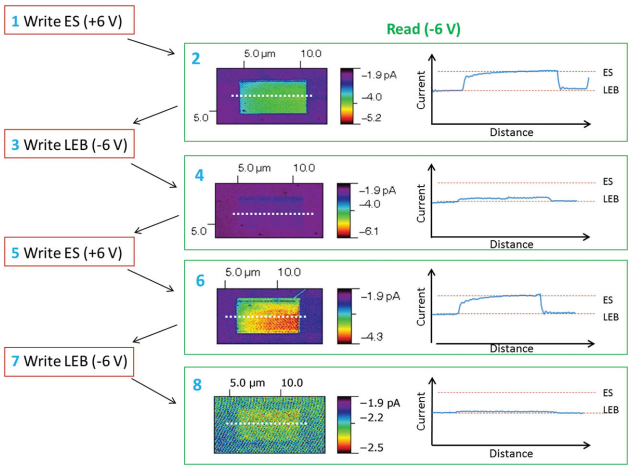

Scheme 2. Schematic of the process used to test the reversibility of the c-AFM reduction reaction, "write" processes are shown in red boxes, "read" in green; numbers in brackets are bias values; line profiles correspond to dotted lines, current scale has been divided through by −1 to give positive current values for line profile data. Higher current indicates higher conductivity.

It is important to note here that carrying out the −6 V imaging (or read) scan reduced the ES state back to the LEB state again. In Step 3, the 15 × 7.5 μm^2 area was rescanned with a −6 V bias to ensure that the area was fully reduced, and then read in Step 4. The erase process was then repeated in Step 5 with a +6 V oxidative bias, with the reading scan (−6 V) of the 15 × 7.5 μm area in Step 6 clearly showing the written feature. Steps 7 and 8 then show the final erase step. The write-erase process is reversible for at least six cycles (six was the maximum attempted) with no topographic or structural alterations to the patterned region of the film evident in AFM topography data. The long-term stability of the patterned regions was not a focus of this study. However, the written structures remained intact, with no signs of deterioration, when left overnight (≈12 h) exposed to the ambient environment.

With applications in mind, a number of crucial factors associated with our cAROW process, including the possibility of fabricating arbitrary patterns, the size limits of the technique, and write speed (thus throughput), were explored (**Figure 2**). The sample stage of our commercial c-AFM setup (see the Experimental Section for more details) was removed and replaced with a pair of closed-loop Attocube nanopositioners (ANPs) driven by an Attocube ECC100 controller (Attocube, Germany). The ANPs provided closed-loop scanning within the XY plane and position commands were sent to the ECC100 controller through custom LabVIEW software (National Instruments, USA).

The scan velocity of the ANPs was 4.5 mm s^{-1} and integrated optical encoders enabled the position of each ANP to be monitored with 1 nm precision. Initial tests using the ANPs to scan the sample underneath the tip (with the tip in contact with the sample, microscope Z-control system active and X–Y scanner turned off) created no changes in the conductance of the film. This observation indicated that the 4.5 mm s^{-1} scan speed of the ANPs exceeded the tip–sample speed at which sufficient electrochemical reactions

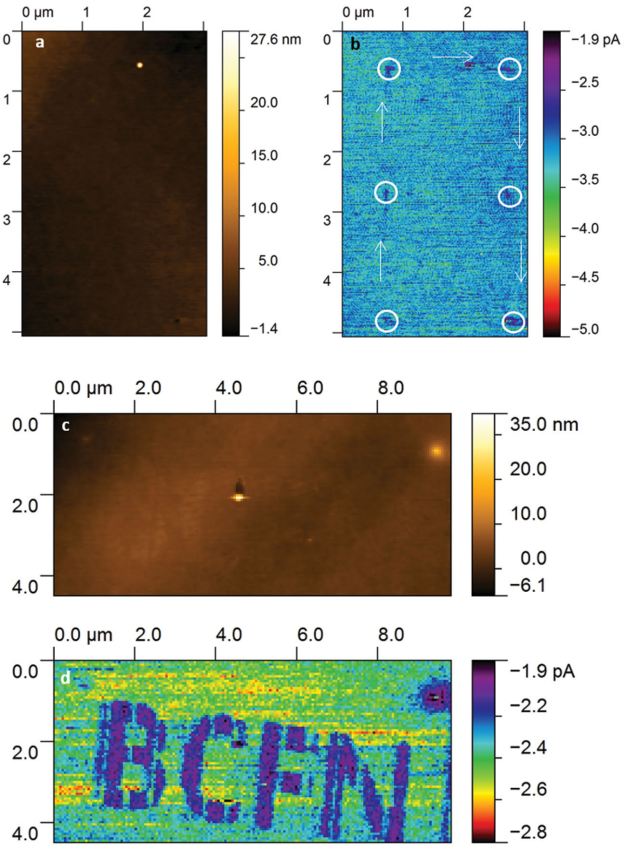

Figure 2. a,b) AFM height and current images of a 3 × 2 array of points written with a 10 ms pause at each point (white circles indicate points, white arrows indicate path of tip across sample); c,d) AFM height and current images of the BCFN logo written with a 100 ms pause at each pixel.

to create a conductance change detectable in the c-AFM signal could take place in the film. Controlling tip–sample speed thus presented a simple method to fabricate patterns on a substrate by (1) scanning at a speed above the threshold speed for writing, then (2) slowing the scan to just below the threshold speed for writing to write a pixel. The ANPs were used to scan the sample across a grid and the ANP paused for a set time (from 10 to 100 ms) at each of an array of points across the scan. The smallest point features were written with a 10 ms pause and were approximately 4 pixels (60 × 60 nm^2) each in the AFM read-back current image (see Figure 2a,b). Longer dwell times of 100 ms yielded repeatable results, and thus used in further investigations (see below).

It is likely that the limiting factor beyond this point is the resolution limit of the detection system used to read back the local state of the thin film, as opposed to a fundamental limit imposed by the mechanism of the fabrication process itself. Improving the write/read resolution was not a focus of this study but it is likely that the optimizations pioneered by researchers studying local oxidation nanolithography, such as using a sharper cantilever tip and faster scan rates,[6,26] should apply here, allowing the fabrication of smaller features. To create arbitrary patterns, bitmap images were converted to (x,y) coordinates, and the ANPs moved to each coordinate

in turn, pausing at each for 100 ms. The microscope was operated in contact mode with a –6 V bias and the Z-feedback loop remained active throughout.

In a final demonstration of the ability of our cAROW technique to write arbitrary patterns at high speed, bitmap images ("BCFN", also "UoB" and "NSQI", see Figure S6, Supporting Information) were converted into sets of coordinates (a coordinate for each pixel) and fabricated with a dwell time per pixel of 100 ms. The results of these scans can be seen in Figure 2c,d and show the expected change in current. Scanning the ANPs with such a high line density began to make physical changes to the film too (the "BCFN" text is just visible in the height image). To demonstrate the repeatability of the writing procedure, the BCFN logo was patterned a further eight times on different areas of the substrate. The current images of each of these eight areas are shown in Figure S5, Supporting Information; in all cases the logo is accurately reproduced and the cAROW procedure functioned as expected.

In summary, we have demonstrated the facile controlled fabrication of arbitrary nanoscale conducting and nonconducting features in an organic semiconductor thin film produced from low molecular weight functional materials. This single-step and facile process is highly reversible and takes place under ambient conditions. While we have demonstrated a small change in a low current, films of TANI derivatives with conductivities as high as 21 mS cm^{-1} have been reported elsewhere. We expect that a library of available TANI-based materials and dopant acids[27] will allow refinement of thin-film fabrication capabilities to give films with substantially higher conductivities. Such high conductivities will clear the path to move away from using conducting substrates—which will make fabricating electronic components a challenge—and lead to a much greater magnitude of difference in conductivity between the LEB and ES states. Likewise, increasing the resolution and write-speed of the process through the use of sharper tips and incorporation into high-speed AFMs,[28–31] as has previously been demonstrated with AFM oxidation of silicon,[19,20] will allow application of this technique. Areas under current consideration for further exploration include detailed electrochemical studies (also on larger patterned areas), careful exploration of a variety of operating conditions to ensure wide applicability, and controlled fabrication of fundamental electronic components such as nanoscale diodes and transistors.

Experimental Section

All experiments were carried out on **TANI-C_8(CSA)$_{0.5}$** films (see Supporting Information) with a Dimension V or Multimode AFM system equipped with the TUNA II module (Bruker, USA). The cantilevers used for these experiments were rectangular Pt/Ir-coated monolithic silicon cantilevers with a spring constant of 0.2 N m^{-1} (CONTPt, NanoWorld, Switzerland). All c-AFM biases quoted refer to sample–tip biases, and the polarity of the current matches the polarity of the imaging bias, so if, for example, a –6 V imaging bias is used, then a higher magnitude current will be more negative.

TANI-C_8 was synthesized using the method reported in the literature.[32] Solutions of CSA-doped **TANI-C_8** were prepared, sonicated and then stirred for 48 h. A drop of 10^{-3} M **TANI-C_8(CSA)$_{0.5}$** octanol solution was drop-cast onto freshly cleaved HOPG heated to ≈ 200 °C and the substrates held at this temperature for a few minutes.

Supporting Information

Supporting Information is available from the Wiley Online Library or from the author.

Acknowledgements

The authors wish to thank Dr. Zhecheng Shao and Mr. Alex Bell for synthesizing the TANI derivatives used in this work and Prof. Walther Schwarzacher for access to his conductive AFM and many helpful discussions. The Microscopy Suite within the School of Chemistry is acknowledged for support. M.J.M. gratefully acknowledges a Royal Society Wolfson Merit Award. B.P.B. acknowledges Bristol Centre for Functional Nanomaterials and the Engineering and Physical Sciences Research Council for funding.

[1] N. Kodera, D. Yamamoto, R. Ishikawa, T. Ando, *Nature* **2010**, *468*, 72.
[2] T. Ando, *Nanotechnology* **2012**, *23*, 062001.
[3] P. Hinterdorfer, Y. F. Dufrêne, *Nat. Methods* **2006**, *3*, 347.
[4] N. G. Walter, C. Bustamante, *Chem. Rev.* **2014**, *114*, 3069.
[5] R. Garcia, R. V. Martinez, J. Martinez, *Chem. Soc. Rev.* **2006**, *35*, 29.
[6] R. V. Martínez, J. Martínez, R. Garcia, *Nanotechnology* **2010**, *21*, 245301.
[7] D. A. Unruh, C. Mauldin, S. J. Pastine, M. Rolandi, J. M. J. Fréchet, *J. Am. Chem. Soc.* **2010**, *132*, 6890.
[8] J. Clausmeyer, J. Henig, W. Schuhmann, N. Plumeré, *ChemPhysChem* **2014**, *15*, 151.
[9] X. Luo, V. A. Pedrosa, J. Wang, *Chem. Eur. J.* **2009**, *15*, 5191.
[10] J. Germain, M. Rolandi, S. A. Backer, J. M. J. Fréchet, *Adv. Mater.* **2008**, *20*, 4526.
[11] J. D. Torrey, S. E. Vasko, A. Kapetanovic, Z. Zhu, A. Scholl, M. Rolandi, *Adv. Mater.* **2010**, *22*, 4639.
[12] R. Garcia, A. W. Knoll, E. Riedo, *Nat. Nanotechnol.* **2014**, *9*, 577.
[13] N. S. Losilla, J. Martinez, E. Bystrenova, P. Greco, F. Biscarini, R. García, *Ultramicroscopy* **2010**, *110*, 729.
[14] R. Garcia, N. S. Losilla, J. Martínez, R. V. Martinez, F. J. Palomares, Y. Huttel, M. Calvaresi, F. Zerbetto, *Appl. Phys. Lett.* **2010**, *96*, 143110.
[15] F. Lopour, R. Kalousek, D. Skoda, J. Spousta, F. Matejka, T. Sikola, *Surf. Interface Anal.* **2002**, *34*, 352.
[16] S. Hoeppener, R. Maoz, J. Sagiv, *Adv. Mater.* **2006**, *18*, 1286.
[17] B. Pignataro, A. Licciardello, S. Cataldo, G. Marletta, *Mater. Sci. Eng. C* **2003**, *23*, 7.
[18] D. Wouters, R. Willems, S. Hoeppener, C. F. J. Flipse, U. S. Schubert, *Adv. Funct. Mater.* **2005**, *15*, 938.
[19] J. A. Vicary, M. J. Miles, *Nanotechnology* **2009**, *20*, 095302.

[20] J. A. Vicary, M. J. Miles, *Ultramicroscopy* **2008**, *108*, 1120.
[21] Z. Wei, C. F. J. Faul, *Macromol. Rapid Commun.* **2008**, *29*, 280.
[22] Z. Shao, P. Rannou, S. Sadki, N. Fey, D. M. Lindsay, C. F. J. Faul, *Chem. Eur. J.* **2011**, *17*, 12512.
[23] Z. Wei, T. Laitinen, B. Smarsly, O. Ikkala, C. F. J. Faul, *Angew. Chem. Int. Ed.* **2005**, *44*, 751.
[24] J. O. Thomas, H. D. Andrade, B. M. Mills, N. A. Fox, H. J. K. Hoerber, C. F. J. Faul, *Small* **2015**, DOI: 10.1002/smll.201500511.
[25] Current–voltage spectroscopy was carried out on as-prepared and modified samples. No consistent, repeatable data could be gathered, possibly due to the low conductivity of the sample, and the results proved inconclusive (see Figure S3, Supporting Information, for example, data).
[26] J. A. Dagata, T. Inoue, J. Itoh, K. Matsumoto, H. Yokoyama, *J. Appl. Phys.* **1998**, *84*, 6891.
[27] B. Dufour, P. Rannou, P. Fedorko, D. Djurado, J.-P. Travers, A. Pron, *Chem. Mater.* **2001**, *13*, 4032.
[28] L. Picco, L. Bozec, A. Ulcinas, D. J. Engledew, M. Antognozzi, M. Horton, M. J. Miles, *Nanotechnology* **2007**, *18*, 044030.
[29] B. P. Brown, L. Picco, M. J. Miles, C. F. J. Faul, *Small* **2013**, *9*, 3201.
[30] F. Iwata, Y. Ohashi, I. Ishisaki, L. M. Picco, T. Ushiki, *Ultramicroscopy* **2013**, *133*, 88.
[31] P. Klapetek, M. Valtr, L. Picco, O. D. Payton, J. Martinek, A. Yacoot, M. J. Miles, *Nanotechnology* **2015**, *26*, 065501.
[32] Z. Shao, Z. Yu, J. Hu, S. Chandrasekaran, D. M. Lindsay, Z. Wei, C. F. J. Faul, *J. Mater. Chem.* **2012**, *22*, 16230.

Received: June 20, 2015
Published online: July 28, 2015

